2022

# Lessons Learned from the Modelling of a Novel Compressor-Expander

Andy Pearson

Jon Fenton

Joe Subert

# Lessons learned from the modelling of a novel compressor-expander

Andy PEARSON[a], Jon FENTON[b], Joe SUBERT[b]

Star Refrigeration Ltd,
Glasgow, United Kingdom
+441416387916, apearson@star-ref.co.uk

## ABSTRACT

A novel design of heat engine, combining beneficial aspects of piston and screw machines is described. The experiences gained in developing performance models of the machine under various operating scenarios are detailed. The advantages and disadvantages of different modelling software packages are discussed, with observations of the ways to get the best out of the models. Some provisional results for the operation of the machine are presented and some suggestions for further development are offered.

## 1. INTRODUCTION

This paper describes the development of a compressor-expander model using a particular brand of software. Throughout the paper this will be referred to as "the modelling software" and unless otherwise stated should be taken to mean the particular package used. Some of the lessons learned may not therefore be transferrable to other packages or systems. The work described here has been conducted from 2018 to the present and is ongoing. It has been applied to the development of a novel turbine which can be used as a compressor or as an expander and can also be configured as a combination of compressor and expander, known as a compander (Fenton et al, 2020), with two halves of the turbine operating in opposition to each other. The modelling described is focused on the compander configuration with two applications in mind; as a refrigerating system and as a heat engine to generate electrical power from waste heat recovery.

## 2. BACKGROUND

The novel turbine was developed by FeTu Ltd and has been found to combine the beneficial features of a reciprocating machine and a screw machine. It comprises a drive shaft incorporating a flat blade and a spherical rotor constrained to pivot relative to the rotating blade, causing chambers between the blade and the sphere to vary in volume. A full description of the device is given in Fenton (2019). Further details of the construction are shown in Figure 1 and Figure 2, which are abstracted from Fenton (2021). For details of the component numbering, refer to the source documents.

The turbine uses positive displacement to compress or expand a working fluid, so it is not analogous to a centrifugal or axial turbine. For simplicity this description is expressed in terms of a compressor but the same considerations apply to the use of the turbine as an expander.

In a reciprocating compressor the piston oscillates within a cylindrical chamber between the maximum volume (at bottom dead centre) and the minimum volume (at top dead centre), giving a swept volume which can be expressed as the cross section of the cylinder multiplied by the stroke of the piston. This gives the advantage of enabling a very high volumetric efficiency to be achieved provided the clearance volume (the volume remaining when the piston is at top dead centre) does not re-expand to fill the cylinder before the next intake of suction gas is admitted to the compression space. There is therefore clearly a relationship between compression ratio and volumetric efficiency. A screw compressor avoids this pitfall by using a motion that progresses continuously without the reversal implicit in the reciprocating motion of the piston. In a screw compressor internal cavities are progressively created, increased in volume to a maximum, reduced in volume and ultimately eliminated. The amount of gas flow is determined by the volume of the internal cavity at the instant that it is isolated from the inlet side of the compressor.

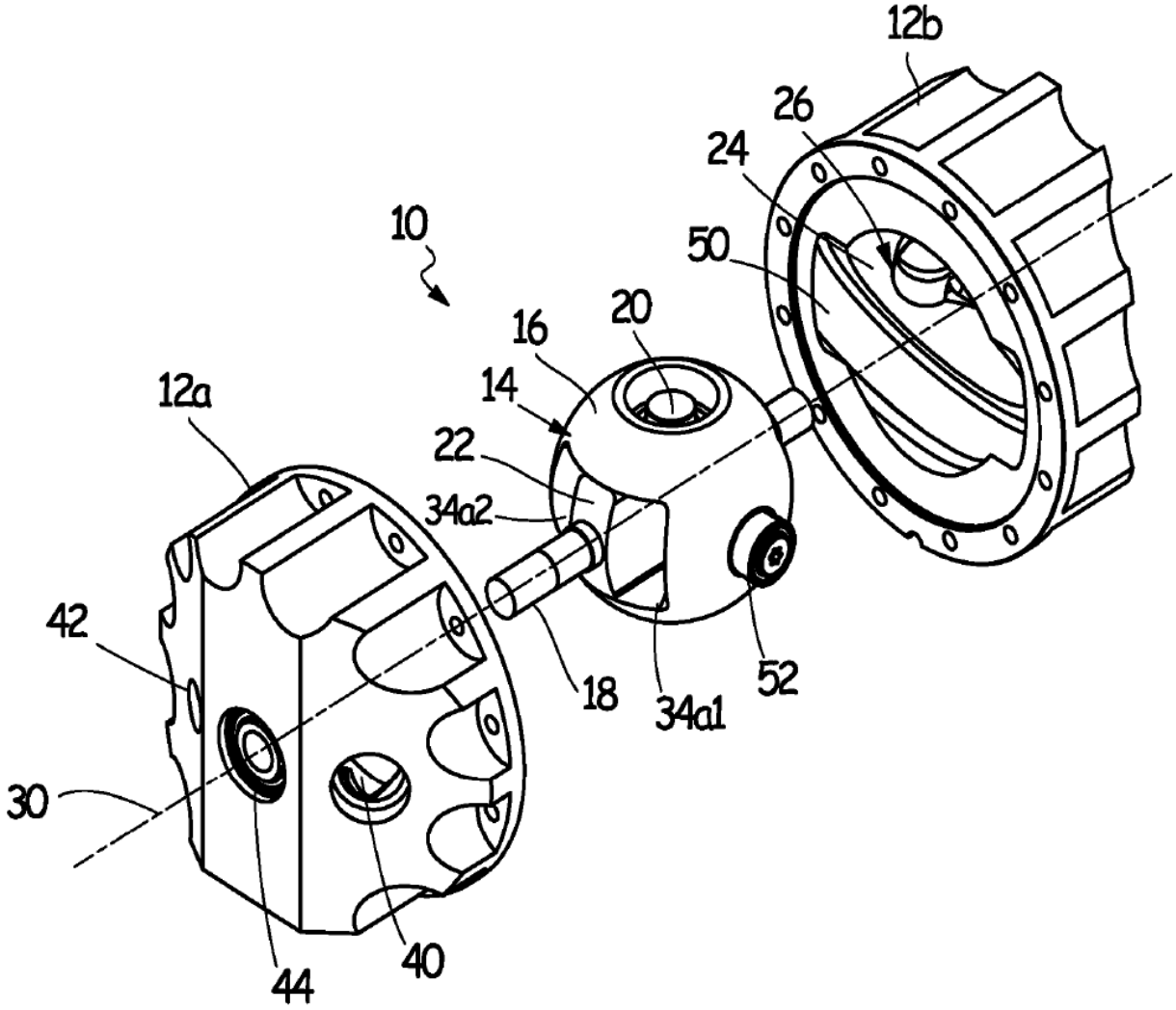


**Figure 1**: an exploded view of the turbine assembly (Fenton, 2021)

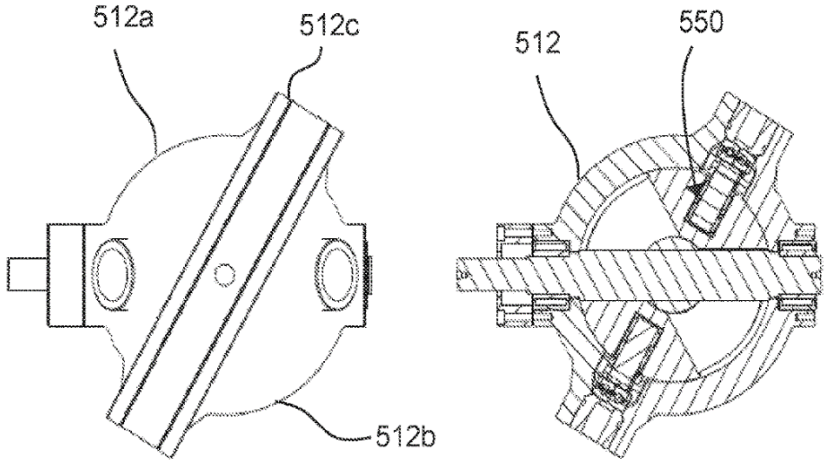


**Figure 2**: elevation and cross section of the turbine assembly (Fenton, 2021)

In Figure 1 it can be seen that there are two compression chambers visible in the exploded view of the turbine, labelled 34a1 and 34a2 on either side of the rotating blade. Figure 2 shows that there are a corresponding pair of chambers on the other side of the spherical rotor. Each pair of chambers can be configured as a compressor or an expander and the volume of the pair of chambers on each side of the spherical rotor can be machined to suit the desired function. Thus both sides can act as compressors, both as expanders or one side as a compressor and one as an expander.

The isentropic efficiency of a screw compressor is determined, among other things, by the ratio between the volume at inlet and the volume at the instant the internal cavity opens to the outlet side of the compressor. The screw compressor therefore has an inherent geometry relating the inlet and outlet volumes, known as the built-in volume ratio (BIVR). In some machines this is adjustable, but for any given BIVR in a screw compressor the optimal isentropic efficiency will be achieved at a corresponding pressure ratio. The volumetric efficiency in a screw compressor, unlike a reciprocating machine, is driven primarily by the pressure difference between inlet and outlet, since this drives the amount of leakage over tip seals and through the gap between the rotors, known as the blowhole.

The novel turbine does not re-expand any residual gas, unlike a reciprocating compressor, but does not have line contact tip seals or a blowhole, unlike a screw compressor so the volumetric efficiency is not impaired by either of these factors and can therefore be extremely high. In early testing of the device with both sides of the rotor configured as a compressor it was noted that the discharge gas temperature was not as high as would be expected in a normal positive displacement compressor. When the machine was run to steady state condition it was found that the temperature of the sphere and the blade remained at a temperature roughly midway between the inlet and discharge temperatures, indicating that there is some inherent cooling mechanism in the operation of the compressor and suggesting that the compression process is somewhere between isentropic compression and isothermal compression. This effect was observed whether both halves of the spherical rotor are used as compression paths or the turbine is configured as a compander.

Early versions of the turbine allowed discharge from the compression chamber across the full sweep of the rotating blade but it was realized that this would not be ideal for use in a power generation cycle so a porting arrangement was introduced whereby the path from the low pressure inlet side and the path to the high pressure outlet side are not opened until the blade is part way through its sweep. This divides the full compression stroke into two distinct phases. The first is quasi-isentropic and the second is quasi-isothermal. Further advantages stem from the quasi-isothermal operation of the turbine. Since the blade and the sphere are maintained at approximately the same temperature it is possible to construct the turbine with much tighter clearances than would otherwise be required to accommodate differential thermal expansion. This in turn enables the sphere and blade to be more robust than would typically be possible in a reciprocating or screw compressor and makes them less susceptible to contamination or distortion. It raises the prospect of arranging for the turbine to operate oil free without incurring significant isentropic or volumetric losses. Although the port arrangement requires complex machining of the casing this is offset by the simplicity of the mechanical drive and the almost complete absence of moving parts.

## 3. DEVELOPING THE MODEL

A model of the turbine was created in 3-D software and imported to various thermodynamic packages to assess their accuracy and ease of use. The models were compared against operating data from a prototype turbine which was run on a university test loop for a brief period. After using several packages for the initial trial, GT Suite from Gamma Technologies was selected because it was relatively easy to use but had sufficient complexity and sophistication to represent the unusual features of the machine. The physical dimensions of the four chambers, including the intake and discharge volumes were modelled as volume curves based on the CAD data at one degree increments. The chambers shown as 34a1 and 34a2 in Figure 1 are 180° out of phase and are matched by two others on the opposite side of the sphere (item 16), although the opposing chambers do not need to be the same size as 34a1 and 34a2. Ingress and discharge from the chambers is through complex shaped ports which are measured from the CAD model and linked to the volume curves. The location of these ports defines the in-chamber volume ratio (ICVR) and determines the compression and expansion ratios achieved by the turbine.

The modelling software enables different degrees of complexity to be switched. This allows rapid prototyping of design changes on an ideal model which is focused on the thermodynamic performance, enabling comparison of outputs on many versions. The preferred solution model can then be re-run allowing for port losses, pipe roughness,

seal losses, rolling bearing losses, inertias, leakages and mechanical losses by switching on those features. This takes much longer to run but gives more realistic results which correlate well with the lab testing that has been done. This two step modelling process also allowed a detailed analysis of operation in oil-free and oil-flooded versions with different clearances in order to assist with the assessment of manufacturing requirements.

To date the modelling has concentrated on the compander version of the turbine where one pair of chambers are configured as compressors and the other as expanders, but some work has also been done with all four chambers as compressors. The main use of the compander has been as a heat engine in these models. Several versions as a refrigeration compressor and refrigeration compander have also been studied. There also appears to be a particular advantage compared with existing technology in using the compander for air-conditioning in air cycle systems and for the use of $CO_2$ as a refrigerant in water chilling applications. Further investigation of these applications is planned.

A diagram of the flow matrix created in the modelling software is shown in Figure 3. This is for a compander in a heat engine system. Note that the network models the complete closed system with the heat source heat exchanger (Q_In_HX) on the left and the heat sink (Q_Out_HX) on the right. The two chambers in the upper portion of the chart (A1b and A1a) are the expanders and the lower chambers (A2a and A2b) are the compressors.

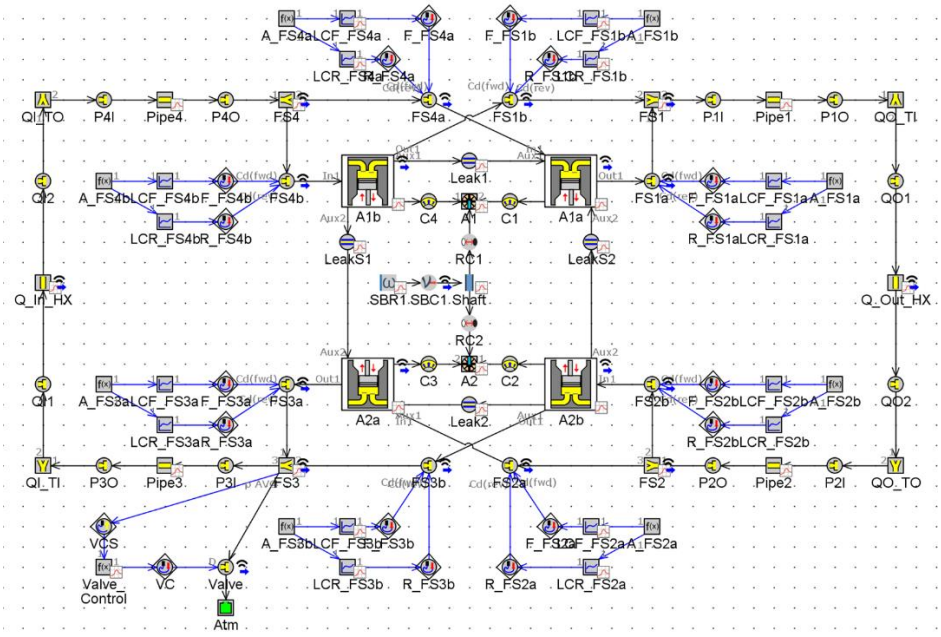


**Figure 3**: Detailed representation of a compander model for heat engine applications

The model includes functional loops at the inlet and outlet of each chamber to reflect the operation of the inlet and outlet ports, allowing a flow coefficient derived from compressor test data and 3D CFD simulations to be used to constrain the gas flow through the port. It simulates leakage between pairs of chambers A1a and A1b (Leak 1) and between A2a and A2b (Leak 2) and also includes leakage along the length of the shaft from A1b to A2a (Leak S1) and from A1a to A2b (Leak S2). All leak paths are bidirectional depending on the pressure difference between the chambers.

Shaft speed, torque and power are derived from a shaft linking chambers A1 (the expander) and A2 (the compressor) and the modelling software enables the speed to be set at a constant value or to be programmed to a fixed pattern, for example a sinusoidal ripple.

The heat exchanger models are kept relatively simple, but they do include inlet and outlet manifold volumes, return bends, parallel flow paths and an internal roughness. This is considered sufficient for the modelling of a system to be built for turbine test purposes but is expected to require further refinement to accurately model behavior of the system for a field application.

The same basic model configuration has been used to investigate work output, refrigeration and heat pump cycles. The software did not require any modification in order to run the model, even though the turbine is not like any conventional compressor or expander.

## 4. RESULTS

An investigation of different two phase fluids in a Rankine cycle heat engine system was conducted. The basic scheme is shown in Figure 4 and the pressure-enthalpy chart for each of the fluids tested is given in Figures 5a to 5f. These are extracted directly from the modelling software. The heat source was at 110°C and the sink was at 10°C. This gives a Carnot conversion ratio, C, of 0.26.

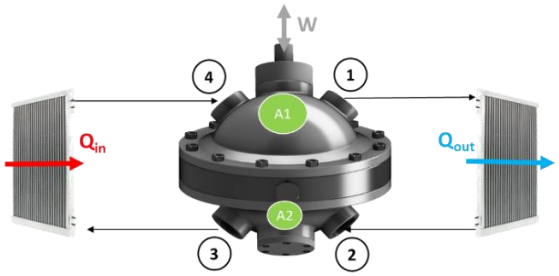


**Figure 4**: simple schematic of a compander system for heat to power applications

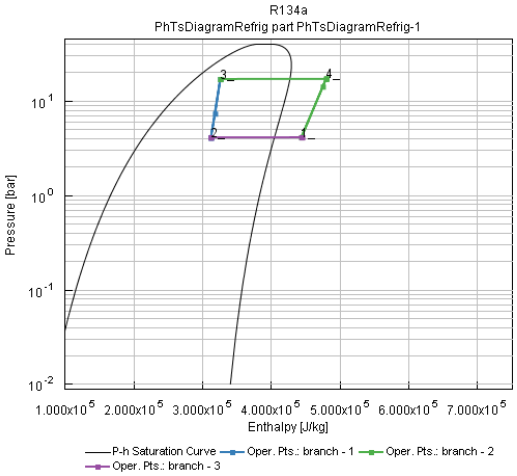


**Figure 5a**: log P-h chart for R-134a

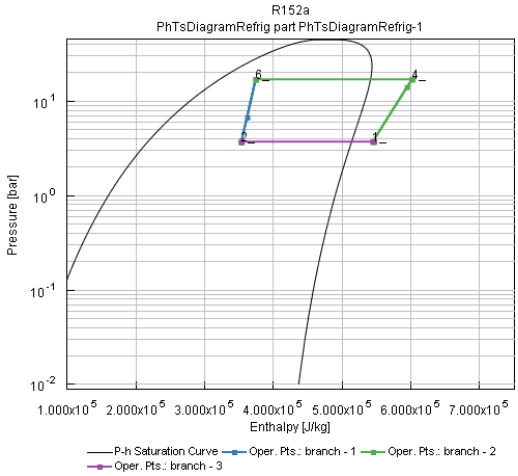


**Figure 5b**: log P-h chart for R-152a

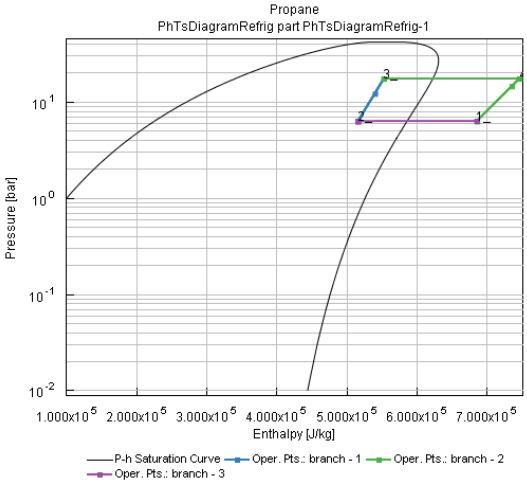


**Figure 5c**: log P-h chart for R-290

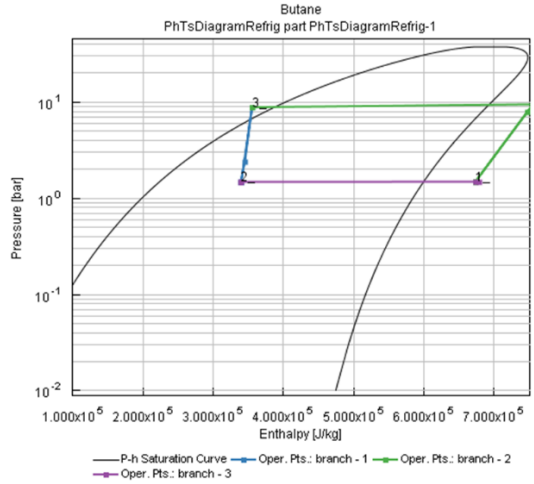


**Figure 5d**: log P-h chart for R-600

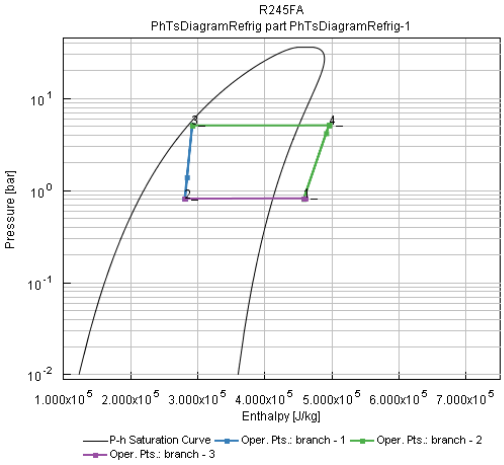


**Figure 5e**: log P-h chart for R-245fa

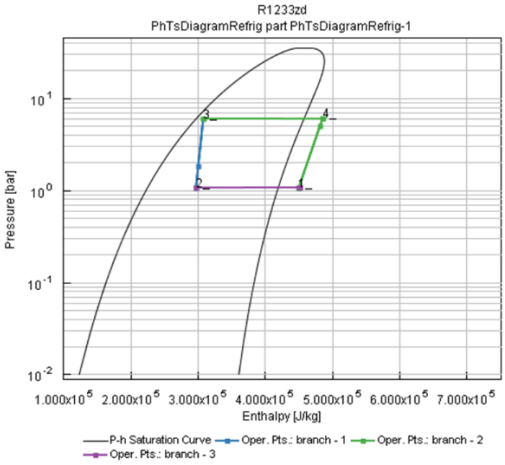


**Figure 5f**: log P-h chart for R-1233zd

The charts illustrate one of the unique features of the turbine, that it can accept significant quantities of liquid in the compressor suction without difficulty. This opens a range of possible systems for the machine where the heat rejection produces only partial condensation of the working fluid. For this exercise the same turbine geometries were used (swept volume and port configuration) and the same precharge pressure applied for R-134a, R-152a, R-290 and R-600, namely 10 bar at 45°C. For the lower pressure fluids R-245fa and R-1233zd a precharge pressure of 5 bar at 80°C to avoid all of the working fluid being condensed before the simulation started. The simulation was also attempted with R-1234yf but it failed to converge. Tests were run with the in-chamber volume (ICVR) ratio ranging from 1.5:1 to 3:1 and with an expander to compressor volume ratio (ECVR) for each fluid of 1.2:1, 1.4:1 and 1.6:1. Simulations with air and carbon dioxide as the working fluid in systems with no phase change were also modelled. Figure 6 shows the ECVR which gave the best actual conversion ratio, C*, for each fluid across the range of ICVRs studied. For reference it is noted that the Carnot conversion ratio, C, for the simulated system was 0.26 and for the two phase fluids the reduced conversion ratio, C', which is calculated from the evaporating and condensing temperatures, varied from fluid to fluid depending on the amount of superheat created in the evaporator prior to the expander inlet. The single phase systems had significantly better values of C* across the range of ICVR tested.

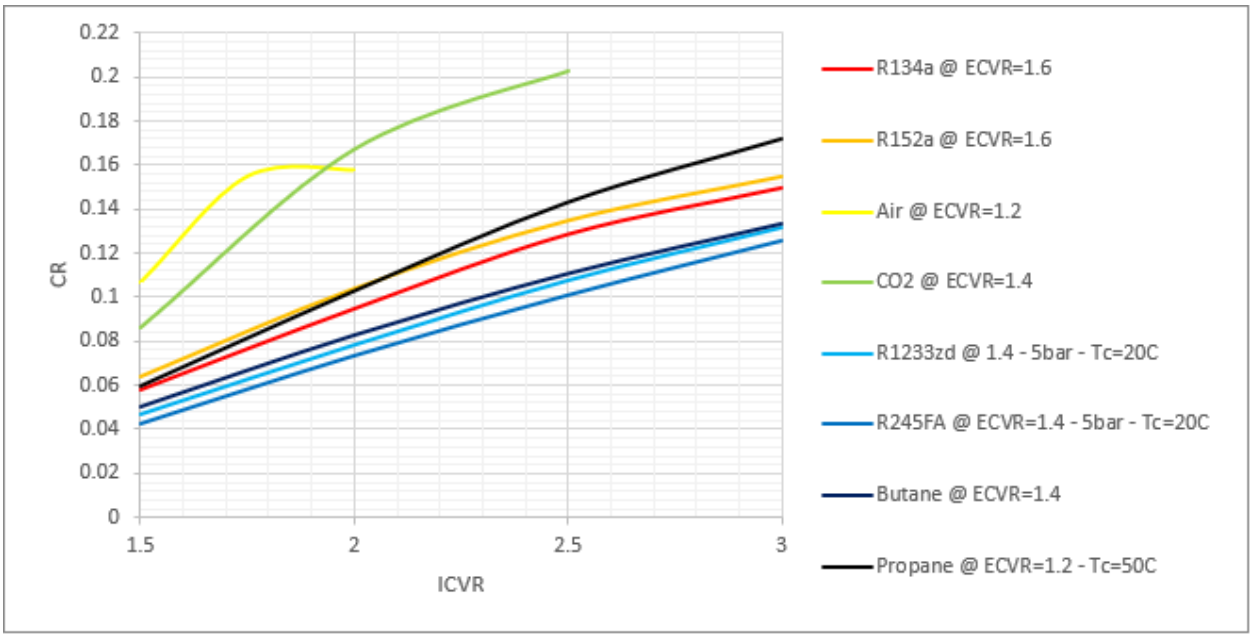


**Figure 6**: heat to power conversion ratio for different working fluids and turbine configurations

Of course the heat conversion ratio is not the whole story. The conditions that allow more heat to be converted also reduce the amount available for conversion so there is a trade off between heat extracted and heat converted.

A reversible cooling and heating system based on the Brayton cycle with air as the working fluid was also investigated. The two configurations are shown in Figures 7a and 7b.


**Figure 7a**: Cooling Mode

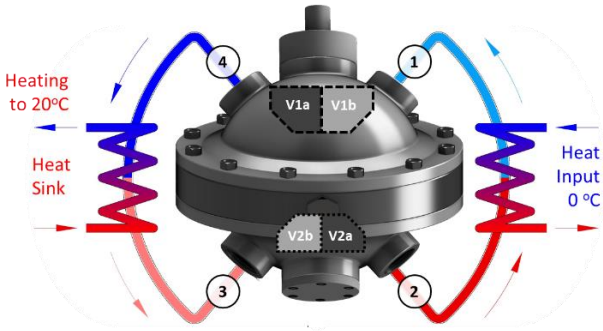


**Figure 7b**: Heating Mode

Five scenarios were modelled. Case 1 and Case 2 had no outlet restriction and expander to compressor volume ratios of 2.4:1 and 1.4:1 respectively. Cases 3 to 5 had shaped outlet ports giving an in-chamber volume ratio of 1.5:1, 2.0:1 and 2.5:1 respectively. The simulation was run in each case with no mechanical losses and then repeated with an allowance for losses. The results for coefficient of performance without losses are shown in Figures 8a (Cooling Mode) and 8b (Heating Mode) and the comparable results with losses are in Figures 9a and 9b.

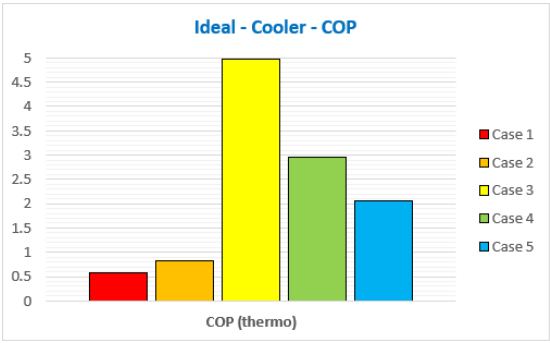


**Figure 8a:** Cooling CoP ($Q_{in}$/W) no losses

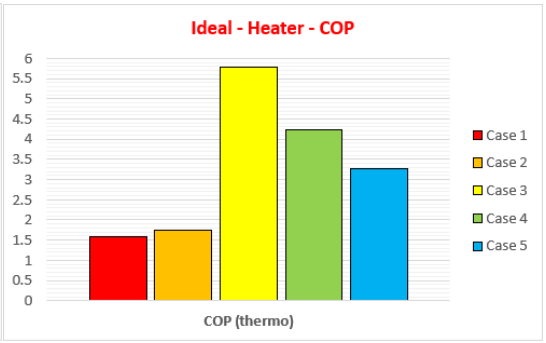


**Figure 8b:** Heating CoP ($Q_{out}$/W) no losses

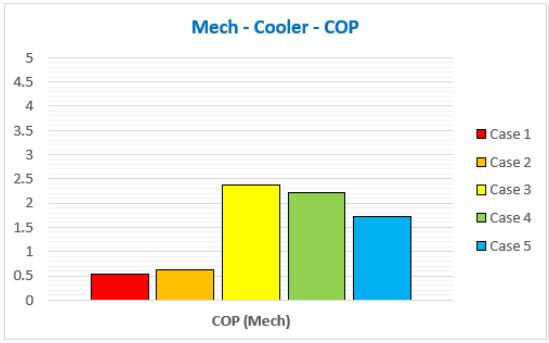


**Figure 9a:** Cooling CoP ($Q_{in}$/W) with losses

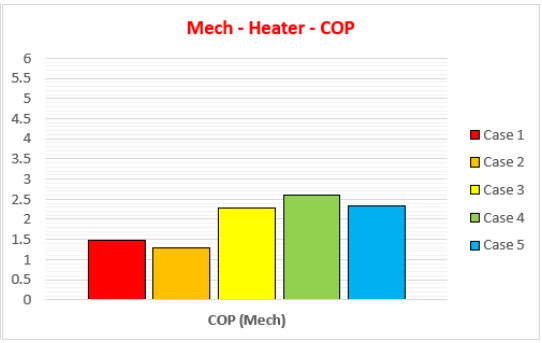


**Figure 9b:** Heating CoP ($Q_{out}$/W) with losses

Although the Case 3 result looked the most promising in the initial study once losses were included it became less attractive than Case 4 and Case 5. The losses comprise friction in the bearings and the guide track. In the oil flooded version there is also a loss associated with moving the oil through the system. There is a significant opportunity to improve the CoP by minimizing these losses compared to those inherent in screw and reciprocating compressors, for example by using low friction magnetic bearings in the guide track (Item 50 in Figure 1).

A good example of the level of detail provided by the model approach adopted is given in Figure 10. This shows traces of instantaneous shaft power over two full revolutions in a heat engine application using air. The red trace shows the theoretical thermodynamic model without losses and the green and blue lines show the power output with and without friction. In this case the friction losses make very little difference to the power output; the difference is about 4.5 kW which matches the validated bearing losses. However, there is a significant fluctuation in the shaft power created by the chambers opening to the external pressure at the end of each compression and expansion stroke. There are two pairs of compression and expansion chambers and they each operate alternately over half a cycle so the pulsations created by ports opening occur twice every revolution.

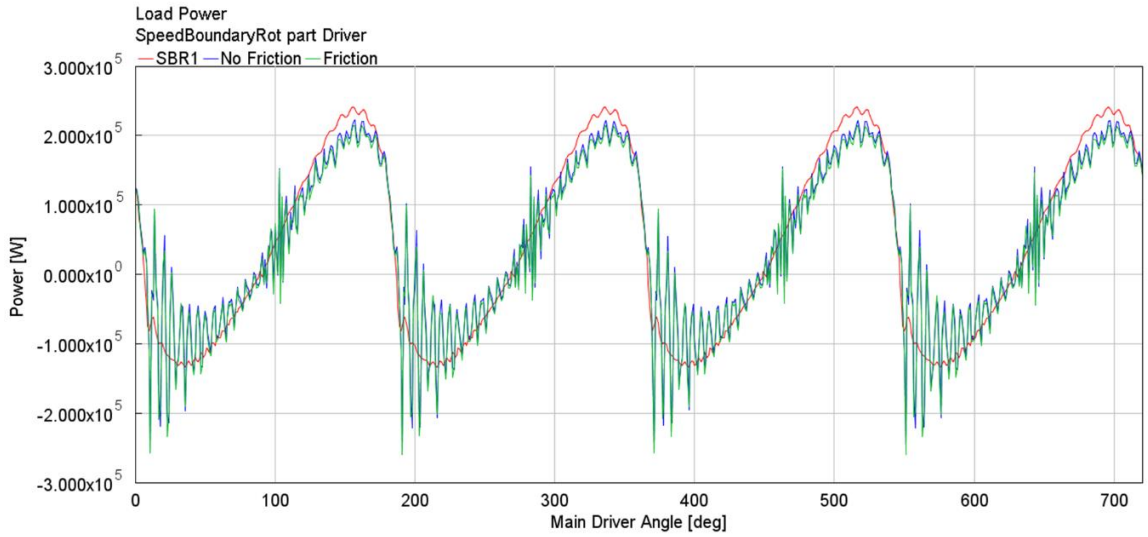


**Figure 10:** Instantaneous power (theoretical and practical) over two revolutions

In Figure 11 the pressures inside both of the compressor and both of the expander chambers are shown. This suggests that the large ripple on the power output is produced when the compressor outlet port opens to high pressure which occurs at driver angles of 0° and 180°. The smaller ripple, which occurs at 90° and 270° happens when the expander outlet port opens to low pressure. In contrast the opening of the port at the beginning of the induction strokes is much smoother. This is because the chamber has zero volume at this point so there is no sudden inrush of air through the port.

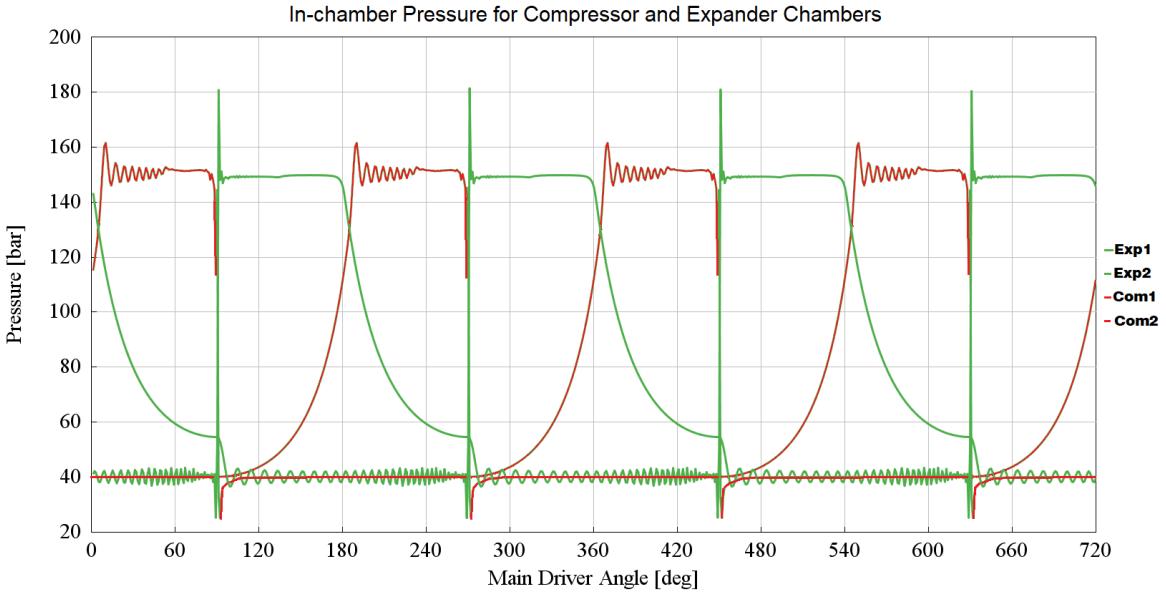


**Figure 11:** In-chamber pressures in the expander and compressor over two revolutions

## 5. CONCLUSIONS

The time spent developing very accurate physical models of the turbine at the beginning of the study has been worthwhile. It has saved much more time in enabling rapid assessment of a large number of variations, including different cycles, different geometries, alternative working fluids, adjustment of port timing, inclusion of oil-flooded operation, different types of bearing and variations in clearances. Running the model without mechanical losses gives fast output and can help to home in on the most suitable arrangements, but as shown in Figures 8 and 9 this can sometimes be misleading so needs to be reviewed periodically by running a more complex model including mechanical losses.

Mechanical testing of the turbine under laboratory conditions provided valuable reference points for bearing losses and leakage which helped to calibrate the model and gave confidence that the test scenarios that could not be validated were also reasonable. Of course other considerations need to be taken into account for physical testing, such as the flammability of the working fluid, the flash point of the lubricant and performance of the shaft seal.

The level of computing power required to run these simulations in reasonable time periods was not available in desktop computers until relatively recently but it is now possible to evaluate a large number of options in the early stages of development to home in on the most promising configurations. However this needs to be done with care. Each step has to be verified as reasonable and feasible, preferably by running simulations several ways and comparing the results to ensure that they are reasonable. It is necessary to understand the physical limitations of the modelling approach. For example where two phase flow is indicated the model may not differentiate between a homogeneous mix of liquid and gas versus two distinct and separate flow regimes.

It must be emphasized that the examples given in this paper do not represent the best results achievable from the developed technology. Rather they were selected because they illustrate a novel aspect of the model, or the degree of precision that can be achieved. These initial results have been used to improve the machine design without incurring the expense of laboratory testing of many variants and the lab tests are now being progressed on the basis of the improved designs resulting from this modelling. The results from the optimized models, however, are less useful for illustrating the benefits of the modelling exercise conducted.

The modelling study gave a clear indication why the performance of Rankine cycle systems falls away so badly as the source temperature reduces. The need for dry expansion predicates a superheated expander inlet condition and the only way to create that superheat is by lowering the evaporating temperature to ensure that there is sufficient temperature difference from the heat source temperature. This does not matter much for high temperature sources, but if the source is only 100 K above the sink then a 15K drop in order to provide 10K superheat has a significant adverse effect on the conversion ratio. This then has the knock on effect of requiring larger ancillary loads for the heat extraction and rejection equipment. There is therefore a double penalty. In contrast, this is not necessary in the single phase systems and the model shows that higher conversion ratios can be achieved with a Brayton cycle than is possible with a Rankine cycle.

## NOMENCLATURE

| | | |
|---|---|---|
| BIVR | Built-in volume ratio | (–) |
| C | Carnot Conversion Ratio | (–) |
| C’ | Reduced Conversion Ratio (the Carnot conversion ratio applied to the difference between evaporating and condensing temperatures) | (–) |
| $C^*$ | Actual Conversion Ratio $W/Q_{in}$ | (–) |
| CoP | Coefficient of Performance | (–) |
| ECVR | Expander:Compressor volume ratio | (–) |
| ICVR | in-chamber volume ratio | (–) |
| Q | Heat transferred | (kW) |
| W | Work transferred | (kW) |

**Subscript**

| | | | |
|---|---|---|---|
| in | from heat or work source | out | to heat or work sink |

## REFERENCES

Fenton, J., (2019) *Roticulating Thermodynamic Apparatus*, WO 2019/166768 A1, World Intellectual Property Organization

Fenton, J., Subert, J., Hinchcliffe, K., Bianchi, G., Tassou, S., (2020) *Air Cycle Feasibility Using a Novel, Single Rotor Compander for Refrigeration and Heating*, DOI: 10.18462/iir.rankine.2020.1167, Proc Int Rankine Conf, IIR, Glasgow

Fenton, J., (2021) *Roticulating Thermodynamic Apparatus*, US 11,805,301 B2, United States Patent and Trademark Office

## ACKNOWLEDGEMENT

The authors would like to thank the directors of FeTu Ltd and Star Refrigeration Ltd for permission to work on this study and publish the findings. Grateful thanks are also due to the staff of Gamma Technologies for their support and encouragement.